F. Toffol, S. Ricci
Wingbox Meta-Model and Aero-Servo-Elastic Optimization With NEOPT
in: International Conference on Multidisciplinary Design Optimization of Aerospace Systems (AeroBest 2021), A.C. Marta, A.Suleman (Eds.), IDMEC, 2021, ISBN: 9789899942486, p. 501-515 [International Conference on Multidisciplinary Design Optimization of Aerospace Systems (AeroBest 2021), Lisbon, Portugal, 21-23 July 2021]

This project has received funding from the Clean Sky 2 Joint Undertaking (JU) under grant agreement No 886552. The JU receives support from the European Union's Horizon 2020 research and innovation programme and the Clean Sky 2 JU members other than the Union.

AeroBest 2021
Lisboa, 21-23 July 2021

WINGBOX META-MODEL AND AERO-SERVO-ELASTIC OPTIMIZATION WITH NEOPT

Francesco Toffol[1]*, Sergio Ricci[1]

1: Department of Science and Technology
Politecnico di Milano
Via La Masa 34, 20156, Milano, Italy
francesco.toffol@polimi.it, sergio.ricci@polimi.it
https://www.aero.polimi.it

Abstract *This work presents a new methodology for the description of the wingbox, suitable for the conceptual and preliminary design phases. Starting from few geometrical information, a semi-analytical model of the wingbox is realized. The wingbox is described with a stick model and its stiffness and mass properties are obtained with a cross-section finite element solver which manages isotropic and orthotropic materials. The beam properties are updated in the aero-elastic model (stick FE +VLM/DLM) which is used for the evaluation of dynamic and trim load envelopes. An optimization framework sizes the wingbox using as design variables its thicknesses, satisfying failure, buckling and flutter constraints.*
The framework is exploited to perform a sensitivity study on a long-haul aircraft, evaluating how different design choices affect the overall performances.

Keywords: Conceptual design, meta-model, multidisciplinary optimization, active control, aero-servo-elasticity

1. INTRODUCTION

Air transportation is an expanding market (+5% per year, pre COVID-19 era [1]), and with the same peace its related emissions are increasing too, recent studies foreseen an outpacing of the CO_2 emission prediction. In the context of an expanding market, aeronautic industries are asked to not only to reduce the greenhouse gases emission, but to invert their trends reaching a carbon neutral aviation by the 2050 [3]. To reach this goal, breakthrough configurations, innovative materials, biofuels and other disruptive solutions must be adopted. Concurrently, design tools must evolve to deal with these new technologies.

The aircraft's range, expressed through the Breguet's equation of Eq.(1), is a performance index which can be used to estimate the efficiency of an aircraft: extending the range with a fixed amount of fuel and payload is equivalent to fly the original range consuming less fuel, hence emitting less CO_2

$$R = \frac{V_{TAS}}{g}\left(\frac{L}{D}\right)\frac{1}{SFC}\,ln\left(\frac{W_{MTOW}}{W_{MTOW} - W_{FUEL}}\right) \tag{1}$$

Breguet's equation clearly identifies three areas that affect the performances of the aircraft and they are the aerodynamic efficiency L/D, the propulsive efficiency expressed through the specific fuel consumption (SFC) and a sort of structural efficiency term related to the initial aircraft mass (W_{MTOW}). Historically, the first improvement in fuel consumption [4] were achieved with the adoption of high bypass ratio (HBPR) engines on the B747 (late '60), in the '80 the diffusion of the computer and computer aided design (CAD) software, for examples in the CFD field [5], led to a new season of efficiency improvement. The latest structural improvements are reached with the adoption of composite materials (e.g. B787 and A350). Nowadays, materials and design methodologies are pushed to their limits, reaching a plateaux in the emissions reduction which can be overcome only adopting new structural configuration like the ultra-high aspect ratio wing (UHARW), the blended wing body (BWB) [6][7][8], the truss-braced wing (TBW) [9], the flying-V [10], the Prandltplane [11][12] and many other exotic ones.

The integrated nature of the aircraft design allows few configurations variation without incurring in multidisciplinary trade-offs, for example increasing the aspect ratio of the wing to achieve better aerodynamic efficiency by reducing the induced drag leads to higher bending moment which requires heavier structures to withstands the increased loads, this is reflected into a reduction of the structural efficiency. The aircraft design is a process where all the disciplines must be considered concurrently, optimizing the overall performance rather than finding the best solution for each field.

The design of a brand-new aircraft is a long and complex process and in the early design phases it is affected by a lot of uncertainty, the situation worsens when disruptive or extreme configurations are considered. The design tools must adapt to this situation, considering new technologies and materials in the design loop, discovering critical areas of the project in early design phases where it is simple and cheap to take mitigation and correction actions to the project, avoiding delay and extra costs.

Historically, the conceptual design tools are still based on statistical or analytical approach for the weight estimation, like the one proposed by Raymer [13] and Torenbeek [14]. These approaches are valid when considering classical tube-wing aluminium alloy configurations, but the spread of new composite materials, extreme configuration and active control technologies limits the validity of these methods.

In the last 15 years new design approaches to the conceptual design were developed:

PROTEUS is the toolbox implemented by TU-Delft [15], the procedure used by Bombardier is described in [16] and the one used by Gulfstresm (ATLASS) can be found in [17]. The Politecnico di Milano Department of Aerospace Science and Technology pioneered this field since the 2007, when it started the development of NeoCASS [18][19][20][21]: it is a Matlab based conceptual design environment, suitable to create low order and medium fidelity analysis models, sized with a physically based method.
NeoCASS performs a full-stress design of a stick FE model with a VLM/DLM aerodynamics, the loads used for the sizing come from aeroelastic trim manoeuvres. The design variables are the thicknesses of the components and through an analytical formulation the beams stiffness and mass matrices are computed. The secondary masses evaluation is performed on the base of statistical methods [22].
NeoCASS has some shortcomings that limit its validity: despite it implements a finite volume beam model [23] that allows to exploit the full beam stiffness matrix (6x6), it computes only the diagonal terms (EA,GA,GJ,EJ) and the extra diagonal terms due to the neutral axis and shear centre offsets with respect to the nodal line, this formulation loses its validity when composite materials are used and the coupling term introduced by them must be considered e.g. to account for the aeroelastic tailoring wash in/out effect.
Moreover, the wingbox's model used in the sizing process is rectangular and symmetric in term of material distribution. Lastly, the sizing is performed considering only static trim manoeuvres, neglecting the dynamic conditions (e.g. gust) and the flutter, which could jeopardize the aircraft safety.
The achievement of the last 70 years in the active control theory and application [25][26] shows how the structural efficiency can be improved by the usage of active technologies.
These aspects must be considered since the early design phases for two reasons: 1) the aero-servo-elastic criticalities must be investigated and faced in the early design phases, where the cost of implementing mitigation and correction actions is still low 2) active control technologies and composite materials must be exploited since this phase to fully take advantage of their potential.
This work proposes a novel aero-servo-elastic optimization framework, named NeOPT, which aims to bridge the gap of NeoCASS's shortcomings. Thanks to development of the wingbox's meta-model, the accuracy of the stick FEM is improved and implemented in an optimization loop able to manage multiple simulations (trim, flutter and dynamic gusts), exploiting composite materials and active control technologies.

2. THE WINGBOX META-MODEL

To provide a better description of the wingbox, the first improvement is related to its geometrical description: NeoCASS and other meta-models, for example the one used in [27], represent the structure with a rectangular section where the spars height is the mean value of the front and rear ones, moreover the skins curvature is not accounted in the properties and stress evaluation. To achieve a better geometrical description of the wingbox, its external surfaces is intersected with a set of planes normal to the beam axis as in Figure 1 (a), which represent the ribs. The obtained ribs outer limits are intersected once more with a set of planes identifying the stringers, which can be parallel to the front or rear spar, or parallel to the beam axis. The result of this intersection procedure is a cloud of 3D points that represents the connection points among the different structural elements as in Figure 1 (b) shows.

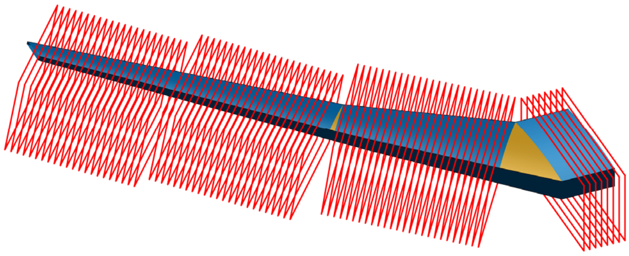

(a) Example of ribs planes

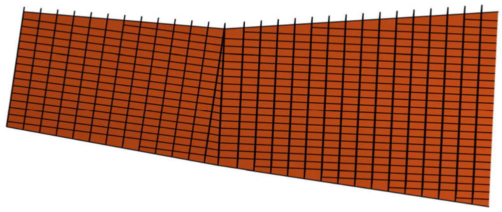

(b) Stringers and ribs skeleton

Figure 1: example of ribs planes and structural elements connection points

The connections among the intersection points identify the structural elements, and their structural properties in term of thickness and material are provided. In this way the wingbox is fully described with a semi-analytical representation called meta-model. The 3D points can be rearranged to obtain different analysis model e.g. by using the connectivity in chord-wise direction it is possible to generate a 2D sectional mesh used by a cross-sectional solver (Figure 2(a)), the overall connectivity generates a detailed 3D FE model of the wingbox with arbitrary mesh refinement along chord, span and spar height (Figure 2(b)).

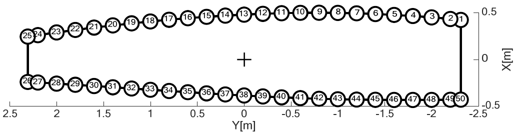

(a) Cross-section 2D mesh

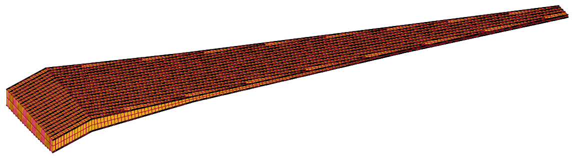

(b) Wingbox 3D FE

Figure 2: models generated by the metamodel.

Another model that can be generated by the meta-model is the CAD of the wingbox in IGES or CATIA format. The pivotal role of the meta-model with respect to the analysis models and results is represented by Figure 3, highlighting how it is more than a simple database of geometrical and structural information, it preserves the analytic connection between heterogenous model without losing information i.e. a modification of a structural properties is automatically mapped in all the domains.

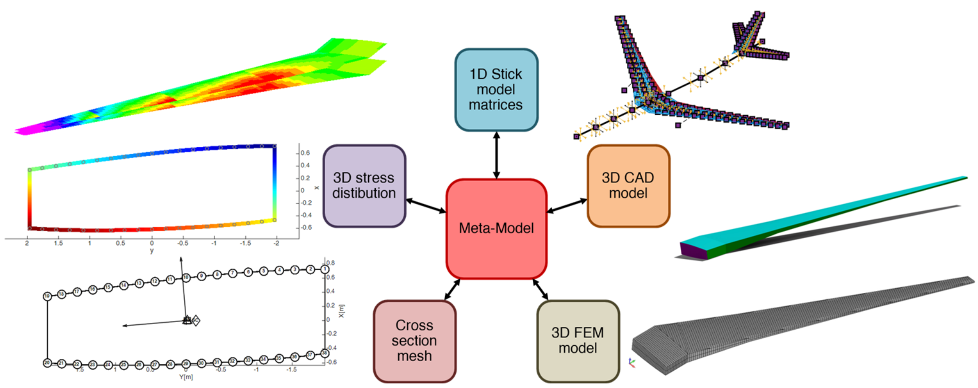

Figure 3: Pivotal role of the meta-model

2.1. NeoANBA

One of the shortcomings of NeoCASS is the lack of accuracy in the correct evaluation of the cross-sectional properties. The terms of the beam matrix are obtained multiplying the geometric properties of the section (A, J, J_t) by the elastic and shear modulus of the material.

$$K = \begin{bmatrix} G \times A_x & & & & & G \times A_x \times X_{SC} \\ & G \times A_y & & & & -G \times A_x \times X_{SC} \\ & & E \times A & -E \times A \times X_{NA} & E \times A \times Y_{NA} & \\ & & & E \times J_{xx} & & \\ & SYM & & & E \times J_{yy} & \\ & & & & & G \times J_t \end{bmatrix} \quad (2)$$

Since an analytic, efficient and accurate method for the evaluation of thin walled and orthotropic hollow section full stiffness matrix is not available, the adoption of a numerical procedure is required. The problem was faced back in the '80, when several models for the cross-section analysis were developed e.g. VABS [28] and ANBA [29], this work follows the approach proposed in the second formulation, calling the new version NeoANBA (NeoCASS + ANBA) [30]. It is a finite elements method cross-sectional solver which assumes that the displacement of a point is described by the sum of a reference line rigid displacement **r** and a warping term **g**, as shown in Figure 4 and described by Eq.(3).

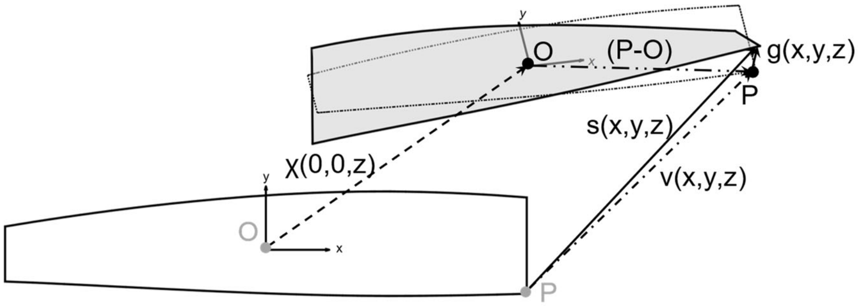

Figure 4: displacement components of a cross section arbitrary point

$$\boldsymbol{S}(x,y,z) = \boldsymbol{\chi}(z) + [(\boldsymbol{P} - \boldsymbol{O}) \times^T]\boldsymbol{\varphi}(z) + \boldsymbol{g}(x,y,z) = \boldsymbol{v}(z) + \boldsymbol{g}(x,y,z) \quad (3)$$

The finite element method is used to approximate the warping field, the unknowns become the warping of the nodes $g = \boldsymbol{Na}$. Exploiting the virtual work principle, it is possible to obtain the description of the internal and external work and to write a linear system which solution provides the cross-section stiffness matrix and the strains, hence stresses through the constitutive law, for unit loads. The current implementation of NeoANBA has only two type of elements: the stringer which considers only the axial stress and the flat panel which considers axial stress and transverse shear, these elements are sufficient to fully characterize the behaviour of a thin walled hollow section.

The full validation and mathematical description can be found in [30]. To demonstrate the capability of the tool, a comparison between the results obtained with a Nastran GFEM and the NeoCASS (meta-model + NeoANBA) is hereafter presented.

The composite rectangular wingbox of Figure 5 is fully realized in unidirectional CFRP and the upper and lower skin's panels have an anti-symmetric orientation of 30° with respect the beam axis.

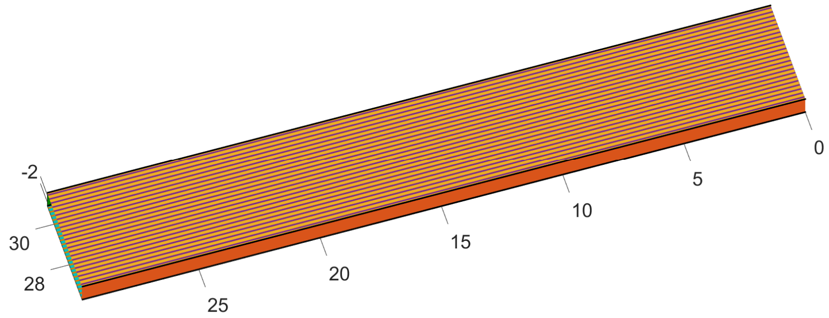

Figure 5: Rectangular wingbox

This kind of lamination creates a bending-torsion coupling, which means that an out of plane bending load, e.g. lift force, generates a torsion around the beam axis and vice-versa.
Figure 6 shows the results in term of displacement obtained for the two models: Figure 6(a) represents the out of plane displacement obtained for an out of plane load (z direction for both load and displacement) and the results obtained are similar, Figure 6(b) shows the rotation around the beam axis obtained for a force in out-of- plane direction (z direction for the force, rotation around y). In this case the discrepancies between the two models are concentrated at the wing root, where the constraints applied to the GFEM stiffen the structure reducing the torsion nearby the clamp, in the spanwise direction the offset between the two models is constant, meaning that the difference is due to a local phenomenon concentrated at the wing root.

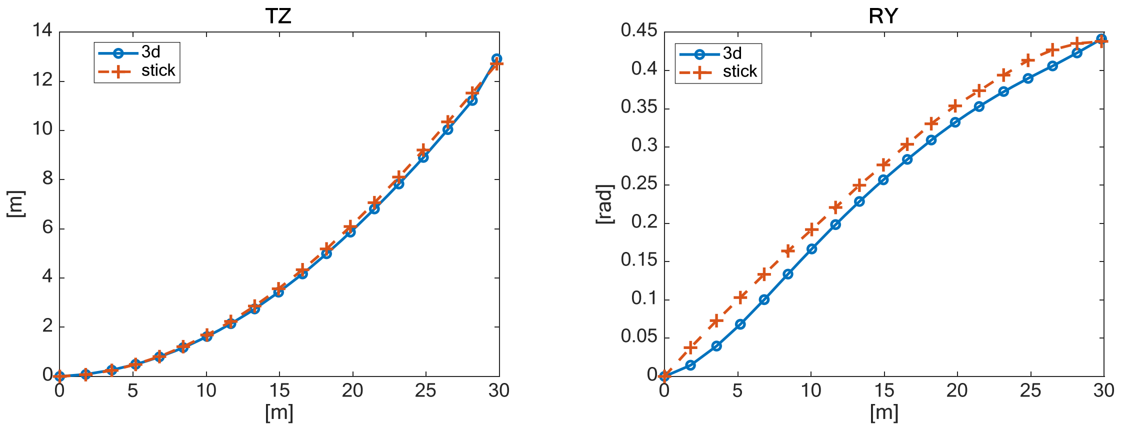

(a) Out of plane displacement for out of plane force

(b) Torsion around beam axis for out of plane force

Figure 6: Bending-coupling effect introduced by anti-symmetric lamination of the skins.

Another quantity which can be recovered by both the models is the stress distribution, represented in Figure 7: the cross-cross section stress distribution obtained with NeoANBA, and expanded in 3D with the meta-model, well matches the one obtained with the GFEM.

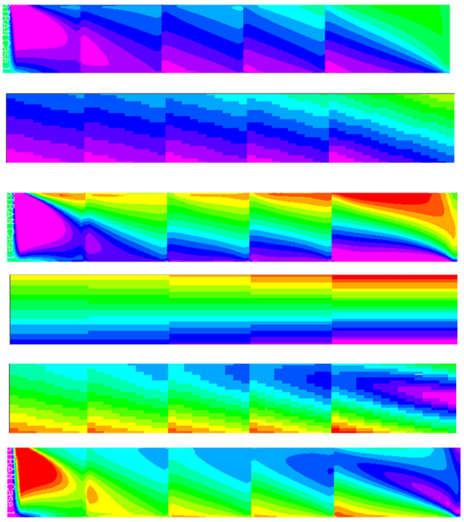

Figure 7: Comparison of the stress distribution

Since the panels used in NeoANBA consider only axial stress and transverse shear, only these components are compared. The global stress pattern is well matched, some discrepancies are present in the boundary regions (constraints and loads) and nearby the properties discontinuity. It must be pointed out that the GFEM is made of more than 20000 nodes while the stick model used by the meta-model has less than 20 nodes.
The proposed meta-model shows how it is possible to improve the characterization of the wingbox without increasing the complexity of the model, providing an improved description of the component which account for the effects introduced by orthotropic materials, exploiting their potential since the early design phases. Moreover, the automatic generation of the detailed 3D FE and CAD models, speeds up the design process providing higher fidelity and ready to use models to the next design phases, without losing the coherence with the stick representation of the aircraft which is still the reference model used for the load envelope computation and aeroelastic simulation.

3. ACTIVE CONTROL

Another important aspect that must be considered in the design process is the interaction between the structures, aerodynamics and control system. The holistic nature of the aero-servo-elasticity suggests that the control system must be designed concurrently to the structure, to fully consider their coupling and exploits possible benefits in term of loads reduction and mass saving. For this reason, an easy but robust and general procedure, suitable to be implemented in an optimization, must be developed. There is a whole literature of methods related to the control of flexible aircraft, but in the conceptual design phases is more important to evaluate the impact of a controller rather than achieve the best performance.
The control design method hereafter proposed is based on the Static Output Feedback structure [31], its simplicity makes this kind of regulator easy to be implemented. The control input **u** is a linear combination of the measure **y**: $\boldsymbol{u} = -\boldsymbol{G}\boldsymbol{y}$, it is a sub-optimal method and there is not an analytical solution for the problem e.g. the Riccati equation for optimal control [32], for this reason the **G** gain matrix must be defined with a numerical procedure.
Among the solutions available in NeoCASS, there is the possibility to realize the State-Space model of the system and operate in continuous time domain [33][34], leading to the representation of Eq.(4).

$$\begin{cases} \dot{x} = Ax + B_u u + B_d d \\ y = C_y x + D_{yu} u + D_{yd} d \\ z = C_z x + D_{zu} u + D_{zd} d \end{cases} \quad (4)$$

The gain matrix is obtained performing an optimization with the Matlab's fmincon, where the design variables are the elements of **G**, the objective function **f** is a weighted sum of the ratio between the closed and open loop performances **z** as in Eq.(5), and the constraints are the stability of the closed loop system and additional user defined and case-specific e.g. the technological limitation of the actuation system.

$$f(x) = \sum_{i=1}^{N} \frac{max\ (|z_i(x,t)|)}{max\ (|z_{io}(x_0,t)|)} \quad (5)$$

The procedure can be exploited to design different controllers for different purposes, like for active flutter suppression (AFS) or a Gust Load Alleviation (GLA). Two applications of the methodology can be found in [30], one applied to the design of a GLA device and another one devoted to the AFS of a wind tunnel model. The results obtained show the soundness of the proposed approach.

4. THE OPTIMIZATION FRAMEWORK

The contents discussed in Sec.2 and Sec.3 enhance the analysis capability of NeoCASS. To fully exploit their potential, they are encompassed in an optimizer named NeOPT. This is a package that performs the refinement of the solution obtained with NeoCASS in the GUESS module, which is used as initial guess. The position of NeOPT inside NeoCASS is illustrated by Figure 8.

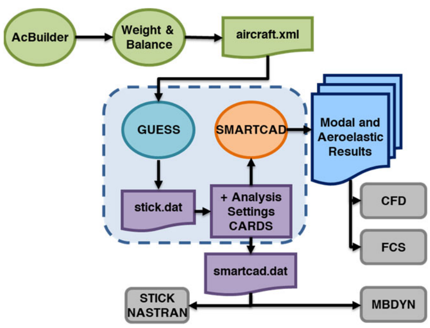

(a)

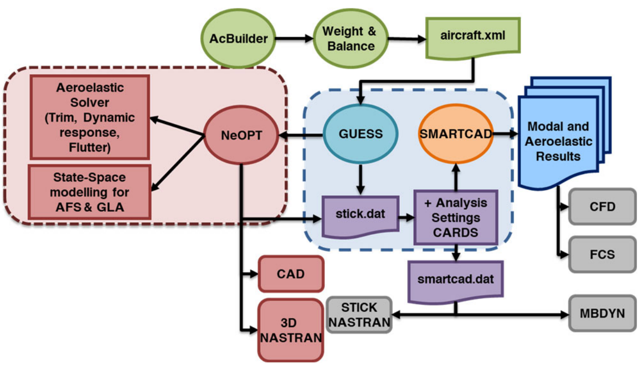

(b)

Figure 8: Difference between NeoCASS standard procedure and NeOPT

The optimizer exploits Matlab's fmincon [35], which is a gradient-based optimizer where the gradient is numerically computed.

The optimization flowchart of the procedure is shown in Figure 10, the design variables of are the thicknesses of the skins, spar webs, spar caps and stringers, the last two have a L and T shape with width and height proportional to the thickness. To limits the number of design variables. a two-level linking strategy is adopted. The first level acts on the cross section, where the user can choose the typology of the section, it can have from 4 to 12 variables: the simplest section has a symmetric distribution of the materials i.e. that the thickness of upper

and lower elements is equal, as well as the front and rear ones. With the increase of the design variables the symmetry is broken, decoupling the thicknesses of the elements. The second linking is performed in spanwise direction: the variables are constant on a user defined patch bounded by two ribs. The number of design variables for the optimization problem is the number of section variables multiplied by the number of patches.
When composite materials are considered, the stacking sequence in term of ply % thickness and orientation are user provided, the only parameters affected by the optimization are the thickness of the laminate and its global orientation with respect to the beam axis.

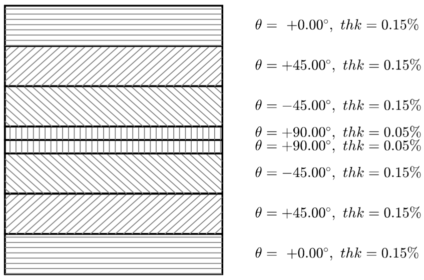

Figure 9: Example of stacking sequence

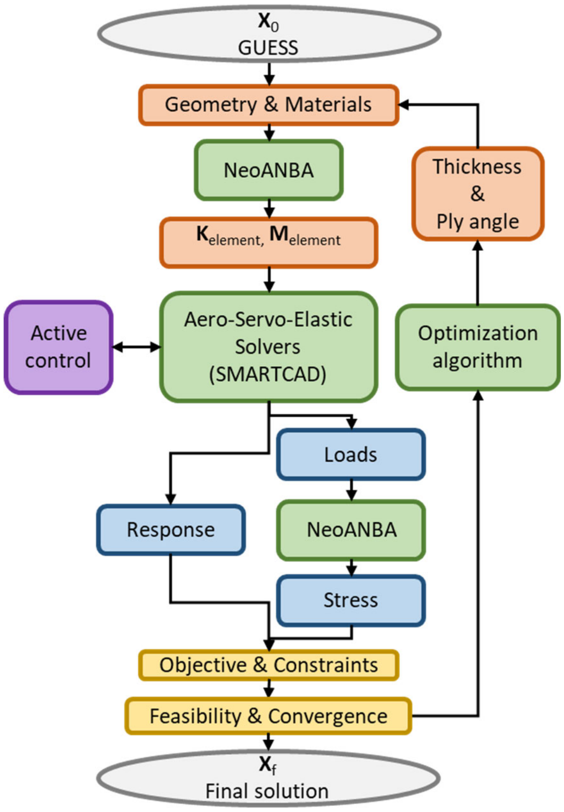

Figure 10: NeOPT flowchart

The constraints imposed to the optimizer are of two types: the first are structural the second are related to analysis response.
The structural constraints impose that no failure nor buckling affect the structure, for both the cases the internal forces obtained with aeroelastic analysis are translated into cross-sectional

stress distribution through the meta-model. The failure of each component is evaluated with the Von Mises criterion for isotropic materials and with the Tsai-Hill criterion for the laminates.
Four buckling mechanisms are considered: single panel buckling, stringer buckling, stringer web buckling and global panel buckling. The analytical approach used is the one described in [36][37] and it allows to deal with iso and orthotropic material in the same way.
Thanks to the opensource nature of the code and to its flexibility, it is possible to use whichever analysis response as objective or as constraint. Typical analysis responses used as constraints are the damping of the aero-elastic modes obtained with flutter solution, which is imposed to be positive across the flight envelope. Other examples of responses that can be considered are the aileron efficiency or the elevator deflection in levelled flight. The default objective function is the mass of the wingbox, but it can be easily modified in whichever available response.
The aeroelastic analyses which can be simultaneously considered in the optimization loop are: trim manoeuvres, flutter and dynamic excitation (gust, control surfaces, external load) with or without the active control.

5. APPLICATION OF NEOPT

The optimizer described in the previous chapter is here exploited to perform a sensitivity and trade-off study on a twin-aisle long-haul (TALH) aircraft, designed from scratch on the basis of the Airbus A330-300 public available data [38] reported in Table 1. The flight envelope consider is represented in Figure 11

Table 1 TAHL general data

Passengers	300
Wing Area	366.7 m^2
Aspect Ratio	9.17
Range 10200 km	(5500Nm)
Max cruise altitude	13100m (43kft)
Max Operative Mach	0.87
Max Operating Speed(EAS)	175m/s (340 kt)
Cabin Altitude	2440m (8000ft)
TAS cruise 38kft	244.91m/s
EAS cruise	127.5m/s
Max CL TO	2.1
Max CL LND	2.5
Clean MAx CL	1.75
Clean CL slope	5.7/rad
Flap TO	15°
Flap LND	25°

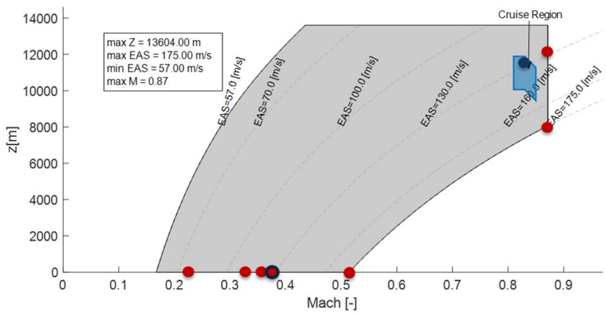

Figure 11 TAHL flight envelope

The objective of the study is to understand how different materials and aspect ratio affect the performance of the aircraft; the wing is stretched keeping fixed its surface to understand how much it is possible to improve the aerodynamic performance without paying too much from the structural point of view. The planar shapes considered and their span values are reported in Figure 12 and Table 2

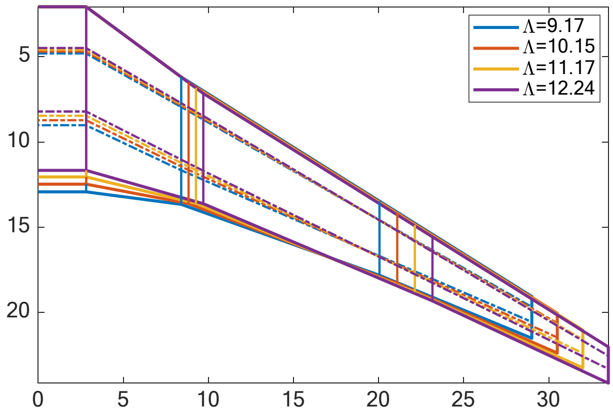

Figure 12: Wings planar shape

Table 2: Wings span and aspect ratio

Span [m]	Λ[-]
58	9.17
61	10.15
64	11.17
67	12.24

The sizing is performed considering 35 trim manoeuvres (push-up, pull down, roll, aileron and elevator deflection, sideslip, etc.) compliant with CS25 regulation and flutter constraints for three altitudes (sea level, corner point and cruise). The evolution of the wingbox mass with respect to the aspect ratio is illustrated in Figure 13 and reported in Table 3.

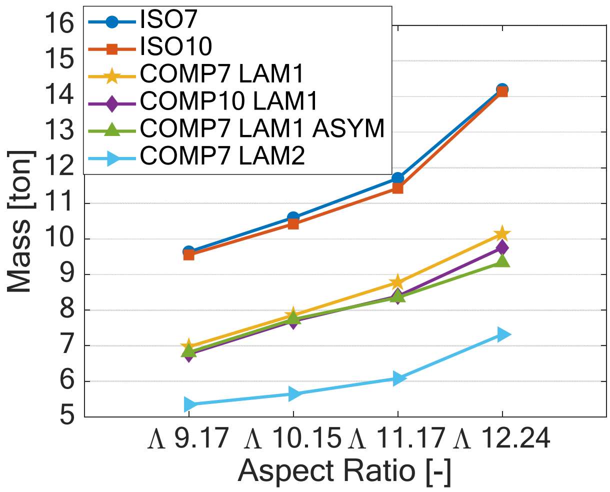

Figure 13: Half wingbox mass variation w.r.t. AR and materials

Table 3: Wingbox mass values

	9.17	10.15	11.17	12.24
ISO7	9639.55	10597.44	11700.06	14200.62
ISO10	9553.53	10418.53	11421.95	13594
COMP7 LAM1	6957.19	7858.91	8778.49	10141.52
COMP10	6770.72	7696.46	8394.62	9751.75
COMP7 LAM1 ASYM	6815.47	7739.76	8357.02	9340.36
COMP7 LAM2	5352.07	5648.47	6081.51	7318.4

The trend shows how a wingspan's increase leads to a heavier structure to withstand higher wing root bending moment, to evaluate if it is worth it an evaluation of the aircraft range and fuel consumption is performed. Both the performances are obtained solving the Breguet equation, in the first case with a fixed amount of fuel in the second case on a prescribed route of 10000km.

$$R = \frac{V_{TAS}}{g} \frac{C_L}{C_{D0} + C_{Di}} \frac{1}{SFC} \ln \frac{W_1}{W_2} \tag{6}$$

The induced drag term is obtained with ALIS [39], a 3D panel method based on Morino's theory. The lift coefficient is the obtained considering a lift equal to the mean value between W_1 and W_2 .

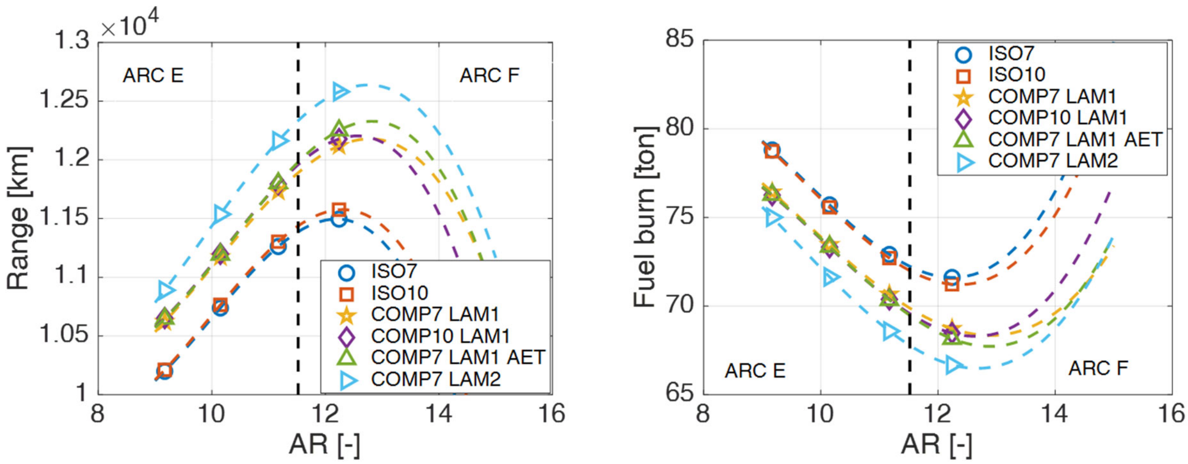

(a) Range (b) Fuel consumption

Figure 14: TAHL performances

The performances obtained show how, for this exercise, the increase of the aspect ratio is convenient for all the material considered, leading to lower fuel consumption. Anyway, some considerations must be done: the big advantage of the composite solution (LAM) is biased by the admissible stresses that are not reduced to consider local effects of fatigue and it may be too optimistic. The effect of aeroelastic tailoring can be noted in Figure 13 and Figure 14: the green triangle markers represent the solution obtained with the same stacking sequence of the yellow star markers, but in the first case (LAM ASYM) the laminate asymmetrical orientation is a design variable and the wash-out effect introduced by the bending-torsion coupling unload the external part of the wing. Figure 14 clearly shows that the AR increase has an optimum point depending on the material, in fact the fuel consumption in function of the AR has a convex shape which minimum can be estimated with a data fitting process. Another important consideration must be done on the span of the aircraft, wingspan larger than 65m requires a modification to the aerodrome reference code (ARC) of the aircraft, requiring different airport infrastructures.

6. CONCLUSIONS

This work proposes a novel aero-servo-elastic optimization toolbox which can be exploited in the early design phases to realize low-order medium fidelity aero-servo-elastic analysis models. The improvement achieved by the meta-model allows to describe the wingbox in a more detailed way, accounting for composite materials and aeroelastic tailoring since the

early design phases.
The proposed active control design methodology is intuitive but robust and it is encompassed in the aero-servo-elastic optimizer, which performs a concurrent optimization of both structure and active control law.
An application of the NeOPT shows a possible exploitation of the toolbox, which helps the designer to understand how design choices affect the overall performances of the aircraft, drawing trends and performing trade-off studies.

7. ACKNOWLEDGMENTS

Part of the activities presented were carried out in the framework of the U-HARWARD Project. This project has received funding from the Clean Sky 2 Joint Undertaking (JU) under grant agreement No 886552. The JU receives support from the European Union's Horizon 2020 research and innovation programme and the Clean Sky 2 JU members other than the Union.

8. DISCLAIMER

The content of this document reflects only the author's view. The European Commission and Clean Sky 2 Joint Undertaking (CS2JU) are not responsible for any use that may be made of the information it contains.

REFERENCES

[1] https://www.iata.org/

[2] H. Tabuchi, "Worse than anyone expected: Air travel emissions vastly outpacepredictions." https://www.nytimes.com/2019/09/19/climate/air-travel-emissions.html, 2019.

[3] E. Commision, "Flightpath 2050 Europe's vision for aviation." https://ec.europa.eu/transport/sites/transport/files/modes/air/doc/flightpath2050.pdf, 2011.

[4] A. Kharina and D. Rutherford, "Fuel efficiency trends for new commercial jet aircraft: 1960 to 2014," 2015

[5] A. Jameson, "Re-engineering the design process through computation," Journal of Aircraft, vol. 36, no. 1, pp. 36–50, 1999.

[6] R. H. Liebeck, "Design of the blended wing body subsonic transport," Journal of aircraft, vol. 41, no. 1, pp. 10–25, 2004.

[7] Z. Lyu and J. R. Martins, "Aerodynamic design optimization studies of a blended-wing-body aircraft," Journal of Aircraft, vol. 51, no. 5, pp. 1604–1617, 2014.

[8] W. Su and C. E. Cesnik, "Nonlinear aeroelasticity of a very flexible blended-wing-body aircraft," Journal of Aircraft, vol. 47, no. 5, pp. 1539–1553, 2010.

[9] R. Jansen, C. Bowman, A. Jankovsky, R. Dyson, and J. Felder, "Overview of nasa electrified aircraft propulsion (eap) research for large subsonic transports," in 53rd AIAA/SAE/ASEE Joint Propulsion Conference, p. 4701, 2017.

[10] T. Delft, "Flying v." https://www.tudelft.nl/en/ae/flying-v/.

[11] A. Frediani, V. Cipolla, and E. Rizzo, "The prandtlplane configuration: overview on

possible applications to civil aviation," Variational Analysis and Aerospace Engineering: Mathematical Challenges for Aerospace Design, pp. 179–210, 2012.

[12] R. Cavallaro, R. Bombardieri, L. Demasi, and A. Iannelli, "Prandtlplane joined wing: Body freedom flutter, limit cycle oscillation and freeplay studies," Journal of Fluids and Structures, vol. 59, pp. 57–84, 2015.

[13] D. Raymer, Aircraft design: a conceptual approach. American Institute of Aeronautics and Astronautics, Inc., 2012.

[14] E. Torenbeek, Synthesis of subsonic airplane design: an introduction to the preliminary design of subsonic general aviation and transport aircraft, with emphasis on layout, aerodynamic design, propulsion and performance. Springer Science & Business Media, 2013.

[15] N. Werter and R. De Breuker, "A novel dynamic aeroelastic framework for aeroelastic tailoring and structural optimisation," Composite Structures, vol. 158, pp. 369–386, 2016.

[16] P. Piperni, A. DeBlois, and R. Henderson, "Development of a multilevel multidisciplinaryoptimization capability for an industrial environment," AIAA journal, vol. 51, no. 10, pp. 2335–2352, 2013.

[17] B. A. Autry and D. Victorazzo, "Automated top level aircraft structural sizing tool (atlass): A framework for preliminary aircraft design and optimization," in AIAA Scitech 2019 Forum, p. 0550, 2019.

[18] L. Cavagna, S. Ricci, and L. Travaglini, "Neocass: an integrated tool for structural sizing, aeroelastic analysis and mdo at conceptual design level," Progress in Aerospace Sciences, vol. 47, no. 8, pp. 621–635, 2011.

[19] L. Cavagna, S. Ricci, and L. Travaglini, "Structural sizing and aeroelastic optimization in aircraft conceptual design using neocass suite," in 13th AIAA/ISSMO Multidisciplinary Analysis Optimization Conference, p. 9076, 2010.

[20] L. Cavagna, S. Ricci, and L. Riccobene, "A fast tool for structural sizing, aeroelastic analysis and optimization in aircraft conceptual design," in 50th AIAA/ASME/ASCE/AHS/ASC Structures, Structural Dynamics, and Materials Conference 17th AIAA/ASME/AHS Adaptive Structures Conference 11th AIAA No, p. 2571, 2009.

[21] L. Cavagna, S. Ricci, and L. Riccobene, "Structural sizing, aeroelastic analysis, and optimization in aircraft conceptual design," Journal of Aircraft, vol. 48, no. 6, pp. 1840–1855, 2011.

[22] Ardema, M. D., Chambers, M. C., Patron, A. P., Hahn, A. S., Miura, H., & Moore, M. D. (1996). Analytical fuselage and wing weight estimation of transport aircraft.

[23] G. L. Ghiringhelli, P. Masarati, and P. Mantegazza, "Multibody implementation of finite volume c beams," AIAA journal, vol. 38, no. 1, pp. 131–138, 2000.

[24] N. Harpur, "The effect of active control systems on structural design criteria," AGARD Active Control Systems for Load Alleviation, Flutter Suppression and Ride Control p 11-22(SEE N74-25550 15-02), 1974

[25] C. D. Regan and C. V. Jutte, "Survey of applications of active control technology for

gust alleviation and new challenges for lighter-weight aircraft," 2012.

[26] E. Livne, "Aircraft active flutter suppression: State of the art and technology maturation needs," Journal of Aircraft, vol. 55, no. 1, pp. 410–452, 2018.

[27] G. Bindolino, G. Ghiringhelli, S. Ricci, and M. Terraneo, "Multilevel structural optimization for preliminary wing-box weight estimation," Journal of Aircraft, vol. 47, no. 2, pp. 475–489, 2010.

[28] Cesnik, C. E., & Hodges, D. H. (1997). VABS: a new concept for composite rotor blade cross-sectional modeling. Journal of the American helicopter society, 42(1), 27-38.

[29] V. Giavotto, M. Borri, P. Mantegazza, G. Ghiringhelli, V. Carmaschi, G. Maffioli, and F. Mussi, "Anisotropic beam theory and applications," Computers & Structures, vol. 16, no. 1-4, pp. 403–413, 1983.

[30] Toffol, F. (2021). Aero-servo-elastic optimization in conceptual and preliminary design.

[31] V. L. Syrmos, C. T. Abdallah, P. Dorato, and K. Grigoriadis, "Static output feedback-a survey," Automatica, vol. 33, no. 2, pp. 125–137, 1997.

[32] Bittanti, S., Laub, A. J., & Willems, J. C. (Eds.). (2012). The Riccati Equation. Springer Science & Business Media.

[33] M. Ripepi and P. Mantegazza, "Improved matrix fraction approximation of aerodynamic transfer matrices," AIAA journal, vol. 51, no. 5, pp. 1156–1173, 2013.

[34] M. Ripepi, Model order reduction for computational aeroelasticity. PhD thesis, Italy, 2014.

[35] T. Mathworks, "Matlab optimization toolbox user's guide," Math Work, 2007.

[36] P. M. Weaver and M. P. Nemeth, "Bounds on flexural properties and buckling response for symmetrically laminated composite plates," Journal of engineering mechanics, vol. 133, no. 11, pp. 1178–1191, 2007.

[37] J. E. Herencia, P. M. Weaver, and M. I. Friswell, "Optimization of long anisotropic laminated fiber composite panels with t-shaped stiffeners," AIAA journal, vol. 45, no. 10, pp. 2497–2509, 2007.

[38] A330-300 triptych from web." https://airbusa330300swissair.blogspot.com/2020/04/airbus-a330-300-technical-specifications.html.

[39] G. Bindolino, P. Mantegazza, and L. Visintini, "A comparison of panel methods for potential flow calculations," in VIII Congresso Nazionale AIDAA, pp. 23–27, 1985.